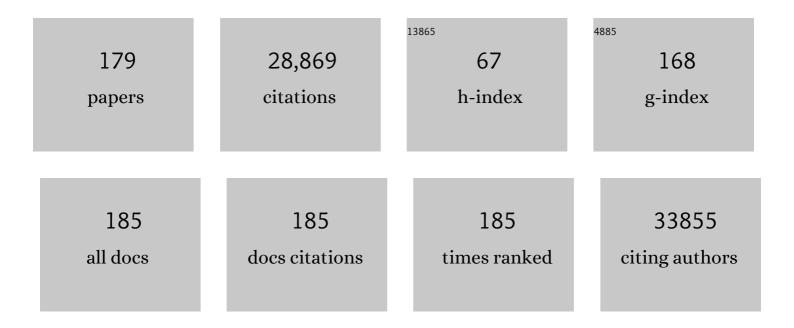


List of Publications by Year in descending order

Source: https://exaly.com/author-pdf/7017407/publications.pdf Version: 2024-02-01



HALLI

#	Article	IF	CITATIONS
1	Chiral cation promoted interfacial charge extraction for efficient tin-based perovskite solar cells. Journal of Energy Chemistry, 2022, 68, 789-796.	12.9	16
2	Single- and few-layer 2H-SnS2 and 4H-SnS2 nanosheets for high-performance photodetection. Chinese Chemical Letters, 2022, 33, 2611-2616.	9.0	3
3	Horseradish peroxidase-triggered direct in situ fluorescent immunoassay platform for sensing cardiac troponin I and SARS-CoV-2 nucleocapsid protein in serum. Biosensors and Bioelectronics, 2022, 198, 113823.	10.1	19
4	Apparent Colors of 2D Materials. Advanced Photonics Research, 2022, 3, 2100221.	3.6	8
5	Ligand-assisted deposition of ultra-small Au nanodots on Fe ₂ O ₃ /reduced graphene oxide for flexible gas sensors. Nanoscale Advances, 2022, 4, 1345-1350.	4.6	7
6	Solvent-Free Preparation of Closely Packed MoS ₂ Nanoscrolls for Improved Photosensitivity. ACS Applied Materials & Interfaces, 2022, 14, 9515-9524.	8.0	10
7	Metallic phase enabling MoS2 nanosheets as an efficient sonosensitizer for photothermal-enhanced sonodynamic antibacterial therapy. Journal of Nanobiotechnology, 2022, 20, 136.	9.1	38
8	Deposition of Vertically Aligned Ag/Ag ₂ S Nanoflakes on EGaIn Particles for Humidity Sensing. Chemistry - A European Journal, 2022, 28, .	3.3	7
9	Direct Synthesis of MoS2 Nanosheets in Reduced Graphene Oxide Nanoscroll for Enhanced Photodetection. Nanomaterials, 2022, 12, 1581.	4.1	6
10	Intralayer Phonons in Multilayer Graphene Moir $ ilde{A}$ © Superlattices. Research, 2022, 2022, .	5.7	4
11	Realization of Oriented and Nanoporous Bismuth Chalcogenide Layers via Topochemical Heteroepitaxy for Flexible Gas Sensors. Research, 2022, 2022, .	5.7	1
12	Defect engineering of layered double hydroxide nanosheets as inorganic photosensitizers for NIR-III photodynamic cancer therapy. Nature Communications, 2022, 13, .	12.8	95
13	Growth of Cu ₂ O Nanoparticles on Two-Dimensional Zr–Ferrocene–Metal–Organic Framework Nanosheets for Photothermally Enhanced Chemodynamic Antibacterial Therapy. Inorganic Chemistry, 2022, 61, 9328-9338.	4.0	55
14	Ternary NiCoTi-layered double hydroxide nanosheets as a pH-responsive nanoagent for photodynamic/chemodynamic synergistic therapy. Fundamental Research, 2022, , .	3.3	3
15	Coplanar Pt/C Nanomeshes with Ultrastable Oxygen Reduction Performance in Fuel Cells. Angewandte Chemie - International Edition, 2021, 60, 6533-6538.	13.8	73
16	A solvent decomposition and explosion approach for boron nanoplate synthesis. Chemical Communications, 2021, 57, 4922-4925.	4.1	3
17	Intrinsic effect of interfacial coupling on the high-frequency intralayer modes in twisted multilayer MoTe ₂ . Nanoscale, 2021, 13, 9732-9739.	5.6	9
18	Heterostructures between a tin-based intermetallic compound and a layered semiconductor for gas sensing. Chemical Communications, 2021, 57, 5590-5593.	4.1	7

#	Article	IF	CITATIONS
19	Coplanar Pt/C Nanomeshes with Ultrastable Oxygen Reduction Performance in Fuel Cells. Angewandte Chemie, 2021, 133, 6607-6612.	2.0	9
20	Activating Layered Metal Oxide Nanomaterials via Structural Engineering as Biodegradable Nanoagents for Photothermal Cancer Therapy. Small, 2021, 17, e2007486.	10.0	94
21	Boosting Electrocatalytic Activity of 3dâ€Block Metal (Hydro)oxides by Ligandâ€Induced Conversion. Angewandte Chemie - International Edition, 2021, 60, 10614-10619.	13.8	101
22	Direct Observation of the Light-Induced Exfoliation of Molybdenum Disulfide Sheets in Water Medium. ACS Nano, 2021, 15, 5661-5670.	14.6	21
23	Amorphization-induced surface electronic states modulation of cobaltous oxide nanosheets for lithium-sulfur batteries. Nature Communications, 2021, 12, 3102.	12.8	103
24	Direct CVD growth of MoS2 on chemically and thermally reduced graphene oxide nanosheets for improved photoresponse. APL Materials, 2021, 9, .	5.1	6
25	Ultraâ€Fast and Scalable Saline Immersion Strategy Enabling Uniform Zn Nucleation and Deposition for Highâ€Performance Znâ€Ion Batteries. Small, 2021, 17, e2101901.	10.0	65
26	Spatially Controlled Preparation of Layered Metallic–Semiconducting Metal Chalcogenide Heterostructures. ACS Nano, 2021, 15, 12171-12179.	14.6	9
27	Wrapping Plasmonic Silver Nanoparticles inside One-Dimensional Nanoscrolls of Transition-Metal Dichalcogenides for Enhanced Photoresponse. Inorganic Chemistry, 2021, 60, 4226-4235.	4.0	17
28	Silicon acid batteries enabled by a copper catalysed electrochemo-mechanical process. Energy and Environmental Science, 2021, 14, 6672-6677.	30.8	2
29	Design of Layerâ€Structured KAlF ₄ :Yb/Er for Pressureâ€Enhanced Upconversion Luminescence. Advanced Optical Materials, 2020, 8, 1901031.	7.3	20
30	Metallic 1T Phase Enabling MoS ₂ Nanodots as an Efficient Agent for Photoacoustic Imaging Guided Photothermal Therapy in the Nearâ€Infraredâ€II Window. Small, 2020, 16, e2004173.	10.0	150
31	Treatment-dependent surface chemistry and gas sensing behavior of the thinnest member of titanium carbide MXenes. Nanoscale, 2020, 12, 16987-16994.	5.6	45
32	Ultrafast Microwave Activating Polarized Electron for Scalable Porous Al toward High-Energy-Density Batteries. Nano Letters, 2020, 20, 8818-8824.	9.1	30
33	Anion-dependent topochemical conversion of CoAl-LDH microplates to hierarchical superstructures of CoOOH nanoplates with controllable orientation. Chemical Communications, 2020, 56, 10285-10288.	4.1	17
34	Few-layer WSe2 lateral homo- and hetero-junctions with superior optoelectronic performance by laser manufacturing. Science China Technological Sciences, 2020, 63, 1531-1537.	4.0	5
35	Amorphous Metal Oxide Nanosheets Featuring Reversible Structure Transformations as Sodium-Ion Battery Anodes. Cell Reports Physical Science, 2020, 1, 100118.	5.6	29
36	Crack Formation on Crystalline Bismuth Oxychloride Thin Square Sheets by Using a Wet hemical Method. ChemNanoMat, 2020, 6, 759-764.	2.8	7

#	Article	IF	CITATIONS
37	Sustainable and Transparent Fish Gelatin Films for Flexible Electroluminescent Devices. ACS Nano, 2020, 14, 3876-3884.	14.6	86
38	Ag@MoS ₂ Core–Shell Heterostructure as SERS Platform to Reveal the Hydrogen Evolution Active Sites of Single-Layer MoS ₂ . Journal of the American Chemical Society, 2020, 142, 7161-7167.	13.7	185
39	Temperature-dependent photoluminescence and time-resolved photoluminescence study of monolayer molybdenum disulfide. Optical Materials, 2020, 107, 110150.	3.6	13
40	Imparting Boron Nanosheets with Ambient Stability through Methyl Group Functionalization for Mechanistic Investigation of Their Lithiation Process. ACS Applied Materials & Interfaces, 2020, 12, 23370-23377.	8.0	15
41	Morphological and Spectroscopic Characterizations of Monolayer and Few-Layer MoS ₂ and WSe ₂ Nanosheets under Oxygen Plasma Treatment with Different Excitation Power: Implications for Modulating Electronic Properties. ACS Applied Nano Materials, 2020, 3, 4218-4230.	5.0	12
42	Scrolling bilayer WS2/MoS2 heterostructures for high-performance photo-detection. Nano Research, 2020, 13, 959-966.	10.4	49
43	Origin of High Efficiency and Long-Term Stability in Ionic Liquid Perovskite Photovoltaic. Research, 2020, 2016345.	5.7	59
44	The influence of two-dimensional organic adlayer thickness on the ultralow frequency Raman spectra of transition metal dichalcogenide nanosheets. Science China Materials, 2019, 62, 181-193.	6.3	5
45	Unconventional solution-phase epitaxial growth of organic-inorganic hybrid perovskite nanocrystals on metal sulfide nanosheets. Science China Materials, 2019, 62, 43-53.	6.3	20
46	Benzodithiophene-modified terpolymer acceptors with reduced molecular planarity and crystallinity: improved performance and stability for all-polymer solar cells. Journal of Materials Chemistry C, 2019, 7, 10338-10351.	5.5	25
47	A Universal Strategy for Stretchable Polymer Nonvolatile Memory via Tailoring Nanostructured Surfaces. Scientific Reports, 2019, 9, 10337.	3.3	15
48	460 DDX5 regulates REG3A mRNA splicing to control wound healing in skin. Journal of Investigative Dermatology, 2019, 139, S79.	0.7	0
49	Engineering the Atomic Layer of RuO ₂ on PdO Nanosheets Boosts Oxygen Evolution Catalysis. ACS Applied Materials & Interfaces, 2019, 11, 42298-42304.	8.0	38
50	Accelerating the startup of microbial fuel cells by facile microbial acclimation. Bioresource Technology Reports, 2019, 8, 100347.	2.7	16
51	Achieving High Volumetric Lithium Storage Capacity in Compact Carbon Materials with Controllable Nitrogen Doping. Advanced Functional Materials, 2019, 29, 1807441.	14.9	39
52	Revisiting the Growth of Black Phosphorus in Sn-I Assisted Reactions. Frontiers in Chemistry, 2019, 7, 21.	3.6	41
53	Silver Nanowireâ€Templated Molecular Nanopatterning and Nanoparticle Assembly for Surfaceâ€Enhanced Raman Scattering. Chemistry - A European Journal, 2019, 25, 10561-10565.	3.3	13
54	Cross-dimensional electron-phonon coupling in van der Waals heterostructures. Nature Communications, 2019, 10, 2419.	12.8	60

#	Article	IF	CITATIONS
55	Ultrafast Cathodic Exfoliation of Few-Layer Black Phosphorus in Aqueous Solution. ACS Applied Nano Materials, 2019, 2, 3793-3801.	5.0	35
56	Impact of pH on Regulating Ion Encapsulation of Graphene Oxide Nanoscroll for Pressure Sensing. Nanomaterials, 2019, 9, 548.	4.1	4
5 7	Oxygen-incorporated MoX (X: S, Se or P) nanosheets via universal and controlled electrochemical anodic activation for enhanced hydrogen evolution activity. Nano Energy, 2019, 62, 338-347.	16.0	102
58	Ethanol Assisted Transfer for Clean Assembly of 2D Building Blocks and Suspended Structures. Advanced Functional Materials, 2019, 29, 1902427.	14.9	14
59	Band Structure Engineering of Interfacial Semiconductors Based on Atomically Thin Lead Iodide Crystals. Advanced Materials, 2019, 31, e1806562.	21.0	79
60	Thick Two-Dimensional Water Film Confined between the Atomically Thin Mica Nanosheet and Hydrophilic Substrate. Langmuir, 2019, 35, 5130-5139.	3.5	4
61	Engineering the Electronic Structure of Submonolayer Pt on Intermetallic Pd ₃ Pb via Charge Transfer Boosts the Hydrogen Evolution Reaction. Journal of the American Chemical Society, 2019, 141, 19964-19968.	13.7	99
62	A general synthesis approach for amorphous noble metal nanosheets. Nature Communications, 2019, 10, 4855.	12.8	321
63	Anisotropic Cu@Cu-BTC core-shell nanostructure for memory device. Chinese Chemical Letters, 2019, 30, 1093-1096.	9.0	3
64	Stable single-atom platinum catalyst trapped in carbon onion graphitic shells for improved chemoselective hydrogenation of nitroarenes. Carbon, 2019, 143, 378-384.	10.3	55
65	Probing interlayer interactions in WSe2-graphene heterostructures by ultralow-frequency Raman spectroscopy. Frontiers of Physics, 2019, 14, 1.	5.0	16
66	Effect of nanostructured silicon on surface enhanced Raman scattering. RSC Advances, 2018, 8, 6629-6633.	3.6	16
67	Ultrathin Palladium Nanomesh for Electrocatalysis. Angewandte Chemie, 2018, 130, 3493-3496.	2.0	24
68	The formation of perovskite multiple quantum well structures for high performance light-emitting diodes. Npj Flexible Electronics, 2018, 2, .	10.7	46
69	Carbon-supported metal single atom catalysts. New Carbon Materials, 2018, 33, 1-11.	6.1	74
70	Ultrathin Palladium Nanomesh for Electrocatalysis. Angewandte Chemie - International Edition, 2018, 57, 3435-3438.	13.8	98
71	Transformable masks for colloidal nanosynthesis. Nature Communications, 2018, 9, 563.	12.8	67
72	Wafer-Scale Ultrathin Two-Dimensional Conjugated Microporous Polymers: Preparation and Application in Heterostructure Devices. ACS Applied Materials & Interfaces, 2018, 10, 4010-4017.	8.0	18

#	Article	IF	CITATIONS
73	Transforming Monolayer Transition-Metal Dichalcogenide Nanosheets into One-Dimensional Nanoscrolls with High Photosensitivity. ACS Applied Materials & Interfaces, 2018, 10, 13011-13018.	8.0	45
74	High phase-purity 1T′-MoS2- and 1T′-MoSe2-layered crystals. Nature Chemistry, 2018, 10, 638-643.	13.6	757
75	Low-temperature photoluminescence emission of monolayer MoS2 on diverse substrates grown by CVD. Journal of Luminescence, 2018, 199, 210-215.	3.1	35
76	Polydopamine Dots-Based Fluorescent Nanoswitch Assay for Reversible Recognition of Glutamic Acid and Al ³⁺ in Human Serum and Living Cell. ACS Applied Materials & Interfaces, 2018, 10, 35760-35769.	8.0	37
77	Perovskite light-emitting diodes based on spontaneously formed submicrometre-scale structures. Nature, 2018, 562, 249-253.	27.8	1,555
78	Realization of vertical metal semiconductor heterostructures via solution phase epitaxy. Nature Communications, 2018, 9, 3611.	12.8	49
79	Crystal phase control in two-dimensional materials. Science China Chemistry, 2018, 61, 1227-1242.	8.2	42
80	Dynamic Ultralong Organic Phosphorescence by Photoactivation. Angewandte Chemie - International Edition, 2018, 57, 8425-8431.	13.8	241
81	A flexible SERS-active film for studying the effect of non-metallic nanostructures on Raman enhancement. Nanoscale, 2018, 10, 16895-16901.	5.6	24
82	Orientation controlled preparation of nanoporous carbon nitride fibers and related composite for gas sensing under ambient conditions. Nano Research, 2017, 10, 1710-1719.	10.4	33
83	Grafting polymerization of singleâ€handed helical poly(phenyl isocyanide)s on graphene oxide and their application in enantioselective separation. Journal of Polymer Science Part A, 2017, 55, 2092-2103.	2.3	14
84	Non onjugated Polymer as an Efficient Dopantâ€Free Holeâ€Transporting Material for Perovskite Solar Cells. ChemSusChem, 2017, 10, 2578-2584.	6.8	64
85	Interdiffusion Reaction-Assisted Hybridization of Two-Dimensional Metal–Organic Frameworks and Ti ₃ C ₂ T _{<i>x</i>} Nanosheets for Electrocatalytic Oxygen Evolution. ACS Nano, 2017, 11, 5800-5807.	14.6	557
86	Scrolling up graphene oxide nanosheets assisted by self-assembled monolayers of alkanethiols. Nanoscale, 2017, 9, 9997-10001.	5.6	16
87	Optical thickness identification of transition metal dichalcogenide nanosheets on transparent substrates. Nanotechnology, 2017, 28, 164001.	2.6	20
88	Composition- and phase-controlled synthesis and applications of alloyed phase heterostructures of transition metal disulphides. Nanoscale, 2017, 9, 5102-5109.	5.6	63
89	Graphene Oxide Scroll Meshes Prepared by Molecular Combing for Transparent and Flexible Electrodes. Advanced Materials Technologies, 2017, 2, 1600231.	5.8	12
90	Nitrogen-enriched pseudographitic anode derived from silk cocoon with tunable flexibility for microbial fuel cells. Nano Energy, 2017, 32, 382-388.	16.0	98

#	Article	IF	CITATIONS
91	Interfacial Interactions in van der Waals Heterostructures of MoS ₂ and Graphene. ACS Nano, 2017, 11, 11714-11723.	14.6	92
92	Solution-processed nitrogen-rich graphene-like holey conjugated polymer for efficient lithium ion storage. Nano Energy, 2017, 41, 117-127.	16.0	159
93	Graphene oxide scroll meshes encapsulated Ag nanoparticles for humidity sensing. RSC Advances, 2017, 7, 40119-40123.	3.6	16
94	Synthesis of WO _{<i>n</i>} â€WX ₂ (<i>n</i> =2.7, 2.9; X=S, Se) Heterostructures for Highly Efficient Green Quantum Dot Lightâ€Emitting Diodes. Angewandte Chemie, 2017, 129, 10622-10626.	2.0	7
95	Synthesis of WO _{<i>n</i>} â€WX ₂ (<i>n</i> =2.7, 2.9; X=S, Se) Heterostructures for Highly Efficient Green Quantum Dot Lightâ€Emitting Diodes. Angewandte Chemie - International Edition, 2017, 56, 10486-10490.	13.8	21
96	Photoluminescence Enhancement Effect of the Layered MoS ₂ Film Grown by CVD. Journal of Engineering (United States), 2017, 2017, 1-8.	1.0	3
97	Ultralow-frequency Raman system down to 10 cmâ^'1 with longpass edge filters and its application to the interface coupling in t(2+2)LGs. Review of Scientific Instruments, 2016, 87, 053122.	1.3	11
98	Strain engineering in monolayer WS2, MoS2, and the WS2/MoS2 heterostructure. Applied Physics Letters, 2016, 109, .	3.3	132
99	Atomically Dispersed Ru on Ultrathin Pd Nanoribbons. Journal of the American Chemical Society, 2016, 138, 13850-13853.	13.7	132
100	Templating C ₆₀ on MoS ₂ Nanosheets for 2D Hybrid van der Waals <i>p</i> – <i>n</i> Nanoheterojunctions. Chemistry of Materials, 2016, 28, 4300-4306.	6.7	58
101	Random terpolymer with a cost-effective monomer and comparable efficiency to PTB7-Th for bulk-heterojunction polymer solar cells. Polymer Chemistry, 2016, 7, 926-932.	3.9	43
102	Self-Assembled Chiral Nanofibers from Ultrathin Low-Dimensional Nanomaterials. Journal of the American Chemical Society, 2015, 137, 1565-1571.	13.7	123
103	Black Phosphorus Quantum Dots. Angewandte Chemie - International Edition, 2015, 54, 3653-3657.	13.8	594
104	A new V-shaped triphenylamine/diketopyrrolopyrrole containing donor material for small molecule organic solar cells. RSC Advances, 2015, 5, 68192-68199.	3.6	16
105	Singleâ€Layer Transition Metal Dichalcogenide Nanosheetâ€Based Nanosensors for Rapid, Sensitive, and Multiplexed Detection of DNA. Advanced Materials, 2015, 27, 935-939.	21.0	322
106	Twoâ€Dimensional CuSe Nanosheets with Microscale Lateral Size: Synthesis and Templateâ€Assisted Phase Transformation. Angewandte Chemie - International Edition, 2014, 53, 5083-5087.	13.8	115
107	Triangular Ag–Pd alloy nanoprisms: rational synthesis with high-efficiency for electrocatalytic oxygen reduction. Nanoscale, 2014, 6, 11738-11743.	5.6	43
108	A Universal, Rapid Method for Clean Transfer of Nanostructures onto Various Substrates. ACS Nano, 2014, 8, 6563-6570.	14.6	192

#	Article	IF	CITATIONS
109	Synthesis of Twoâ€Dimensional Transitionâ€Metal Phosphates with Highly Ordered Mesoporous Structures for Lithiumâ€Ion Battery Applications. Angewandte Chemie - International Edition, 2014, 53, 9352-9355.	13.8	128
110	Coating Two-Dimensional Nanomaterials with Metal–Organic Frameworks. ACS Nano, 2014, 8, 8695-8701.	14.6	168
111	Fabrication of Ultralong Hybrid Microfibers from Nanosheets of Reduced Graphene Oxide and Transitionâ€Metal Dichalcogenides and their Application as Supercapacitors. Angewandte Chemie - International Edition, 2014, 53, 12576-12580.	13.8	119
112	Graphene Oxide Architectures Prepared by Molecular Combing on Hydrophilicâ€Hydrophobic Micropatterns. Small, 2014, 10, 2239-2244.	10.0	23
113	Copperâ€Based Ternary and Quaternary Semiconductor Nanoplates: Templated Synthesis, Characterization, and Photoelectrochemical Properties. Angewandte Chemie - International Edition, 2014, 53, 8929-8933.	13.8	118
114	Liquid-phase growth of platinum nanoparticles on molybdenum trioxide nanosheets: an enhanced catalyst with intrinsic peroxidase-like catalytic activity. Nanoscale, 2014, 6, 12340-12344.	5.6	82
115	Preparation and Applications of Mechanically Exfoliated Single-Layer and Multilayer MoS ₂ and WSe ₂ Nanosheets. Accounts of Chemical Research, 2014, 47, 1067-1075.	15.6	1,374
116	A Solutionâ€Processed Hole Extraction Layer Made from Ultrathin MoS ₂ Nanosheets for Efficient Organic Solar Cells. Advanced Energy Materials, 2013, 3, 1262-1268.	19.5	231
117	Layer Thinning and Etching of Mechanically Exfoliated MoS ₂ Nanosheets by Thermal Annealing in Air. Small, 2013, 9, 3314-3319.	10.0	229
118	Rapid and Reliable Thickness Identification of Two-Dimensional Nanosheets Using Optical Microscopy. ACS Nano, 2013, 7, 10344-10353.	14.6	359
119	Modulating electronic transport properties of MoS2 field effect transistor by surface overlayers. Applied Physics Letters, 2013, 103, .	3.3	88
120	Interlayer Breathing and Shear Modes in Few-Trilayer MoS ₂ and WSe ₂ . Nano Letters, 2013, 13, 1007-1015.	9.1	576
121	Investigation of MoS ₂ and Graphene Nanosheets by Magnetic Force Microscopy. ACS Nano, 2013, 7, 2842-2849.	14.6	117
122	Mechanical Exfoliation and Characterization of Single―and Few‣ayer Nanosheets of WSe ₂ , TaS ₂ , and TaSe ₂ . Small, 2013, 9, 1974-1981.	10.0	544
123	Single-Layer MoS ₂ -Based Nanoprobes for Homogeneous Detection of Biomolecules. Journal of the American Chemical Society, 2013, 135, 5998-6001.	13.7	995
124	Plasmonic enhancement of photocurrent in MoS2 field-effect-transistor. Applied Physics Letters, 2013, 102, .	3.3	201
125	A Bioâ€inspired Platform to Modulate Myogenic Differentiation of Human Mesenchymal Stem Cells Through Focal Adhesion Regulation. Advanced Healthcare Materials, 2013, 2, 442-449.	7.6	40
126	Graphene Oxide Scrolls on Hydrophobic Substrates Fabricated by Molecular Combing and Their Application in Gas Sensing. Small, 2013, 9, 382-386.	10.0	57

#	Article	IF	CITATIONS
127	VAULT PROTEIN-TEMPLATED ASSEMBLIES OF NANOPARTICLES. Nano, 2012, 07, 1250001.	1.0	2
128	Surface Modification of Smooth Poly(<scp>l</scp> -lactic acid) Films for Gelatin Immobilization. ACS Applied Materials & Interfaces, 2012, 4, 687-693.	8.0	38
129	Facile growth of a single-crystal pattern: a case study of HKUST-1. Chemical Communications, 2012, 48, 11901.	4.1	10
130	Molecular Mechanism of Surface-Assisted Epitaxial Self-Assembly of Amyloid-like Peptides. ACS Nano, 2012, 6, 9276-9282.	14.6	29
131	Fabrication of Single―and Multilayer MoS ₂ Filmâ€Based Fieldâ€Effect Transistors for Sensing NO at Room Temperature. Small, 2012, 8, 63-67.	10.0	1,346
132	Optical Identification of Single―and Few‣ayer MoS ₂ Sheets. Small, 2012, 8, 682-686.	10.0	290
133	Goldâ€Nanoparticleâ€Embedded Polydimethylsiloxane Elastomers for Highly Sensitive Raman Detection. Small, 2012, 8, 1336-1340.	10.0	72
134	Fabrication of Flexible MoS ₂ Thinâ€Film Transistor Arrays for Practical Gasâ€5ensing Applications. Small, 2012, 8, 2994-2999.	10.0	817
135	Surface-Enhanced Raman Scattering of Ag–Au Nanodisk Heterodimers. Journal of Physical Chemistry C, 2012, 116, 10390-10395.	3.1	31
136	Single-Layer MoS ₂ Phototransistors. ACS Nano, 2012, 6, 74-80.	14.6	3,103
137	A Universal Method to Produce Low–Work Function Electrodes for Organic Electronics. Science, 2012, 336, 327-332.	12.6	1,878
138	High-density metallic nanogaps fabricated on solid substrates used for surface enhanced Raman scattering. Nanoscale, 2012, 4, 860-863.	5.6	43
139	Fabrication of Graphene Nanomesh by Using an Anodic Aluminum Oxide Membrane as a Template. Advanced Materials, 2012, 24, 4138-4142.	21.0	183
140	Graphene Oxide as a Novel Nanoplatform for Enhancement of Aggregationâ€Induced Emission of Silole Fluorophores. Advanced Materials, 2012, 24, 4191-4195.	21.0	85
141	Peptide Self-Assembly on Mica under Ethanol-Containing Atmospheres: Effects of Ethanol on Epitaxial Growth of Peptide Nanofilaments. Journal of Physical Chemistry B, 2012, 116, 2927-2933.	2.6	15
142	Growth of Large-Area and Highly Crystalline MoS ₂ Thin Layers on Insulating Substrates. Nano Letters, 2012, 12, 1538-1544.	9.1	1,749
143	Mesoscopic organic nanosheets peeled from stacked 2D covalent frameworks. Chemical Communications, 2011, 47, 7365.	4.1	17
144	Nanoparticle-coated PDMS elastomers for enhancement of Raman scattering. Chemical Communications, 2011, 47, 8560.	4.1	69

#	Article	IF	CITATIONS
145	Surface enhanced Raman scattering of Ag or Au nanoparticle-decorated reduced graphene oxide for detection of aromatic molecules. Chemical Science, 2011, 2, 1817.	7.4	249
146	Single-layer graphene oxide sheet: a novel substrate for dip-pen nanolithography. Chemical Communications, 2011, 47, 10070.	4.1	16
147	Confined Water Nanofilm Promoting Nonenzymatic Degradation of DNA Molecules. Journal of Physical Chemistry B, 2011, 115, 2754-2758.	2.6	7
148	Transparent, Flexible, All-Reduced Graphene Oxide Thin Film Transistors. ACS Nano, 2011, 5, 5038-5044.	14.6	305
149	Nanoscaleâ€Controlled Enzymatic Degradation of Poly(<scp>L</scp> â€lactic acid) Films Using Dipâ€Pen Nanolithography. Small, 2011, 7, 226-229.	10.0	24
150	Bottomâ€Up Preparation of Porous Metalâ€Oxide Ultrathin Sheets with Adjustable Composition/Phases and Their Applications. Small, 2011, 7, 3458-3464.	10.0	55
151	A Graphene–Conjugated Oligomer Hybrid Probe for Lightâ€Up Sensing of Lectin and <i>Escherichia Coli</i> . Advanced Materials, 2011, 23, 4386-4391.	21.0	141
152	Triple‣ayer (Au@Perylene)@Polyaniline Nanocomposite: Unconventional Growth of Faceted Organic Nanocrystals on Polycrystalline Au. Angewandte Chemie - International Edition, 2011, 50, 9898-9902.	13.8	55
153	Synthesis of Gold Squareâ€like Plates from Ultrathin Gold Square Sheets: The Evolution of Structure Phase and Shape. Angewandte Chemie - International Edition, 2011, 50, 12245-12248.	13.8	121
154	Singleâ€Layer Semiconducting Nanosheets: Highâ€Yield Preparation and Device Fabrication. Angewandte Chemie - International Edition, 2011, 50, 11093-11097.	13.8	1,517
155	Microstructure – cyclic deformation property relationships of biodegradable di-crystalline triblock copolymers. Polymer, 2011, 52, 3451-3459.	3.8	5
156	The Molecular Basis of Distinct Aggregation Pathways of Islet Amyloid Polypeptide. Journal of Biological Chemistry, 2011, 286, 6291-6300.	3.4	104
157	Polyphenylene Dendrimerâ€Templated In Situ Construction of Inorganic–Organic Hybrid Riceâ€Shaped Architectures. Advanced Functional Materials, 2010, 20, 43-49.	14.9	32
158	Allâ€Carbon Electronic Devices Fabricated by Directly Grown Singleâ€Walled Carbon Nanotubes on Reduced Graphene Oxide Electrodes. Advanced Materials, 2010, 22, 3058-3061.	21.0	201
159	Amphiphilic Graphene Composites. Angewandte Chemie - International Edition, 2010, 49, 9426-9429.	13.8	325
160	Surfaceâ€Induced Synthesis and Selfâ€Assembly of Metal Suprastructures. Small, 2010, 6, 2708-2715.	10.0	10
161	Conjugatedâ€Polyelectrolyteâ€Functionalized Reduced Graphene Oxide with Excellent Solubility and Stability in Polar Solvents. Small, 2010, 6, 663-669.	10.0	278
162	Adhesion, proliferation, and gene expression profile of human umbilical vein endothelial cells cultured on bilayered polyelectrolyte coatings composed of glycosaminoglycans. Biointerphases, 2010, 5, FA53-FA62.	1.6	17

#	Article	IF	CITATIONS
163	Mechanical Manipulation Assisted Self-Assembly To Achieve Defect Repair and Guided Epitaxial Growth of Individual Peptide Nanofilaments. ACS Nano, 2010, 4, 5791-5796.	14.6	30
164	Nanolithography of Single-Layer Graphene Oxide Films by Atomic Force Microscopy. Langmuir, 2010, 26, 6164-6166.	3.5	68
165	Immobilization of Recombinant Vault Nanoparticles on Solid Substrates. ACS Nano, 2010, 4, 1417-1424.	14.6	16
166	Aminosilane Micropatterns on Hydroxyl-Terminated Substrates: Fabrication and Applications. Langmuir, 2010, 26, 5603-5609.	3.5	98
167	Supramolecular Structures of Amyloid-Related Peptides in an Ambient Water Nanofilm. Journal of Physical Chemistry B, 2010, 114, 15759-15765.	2.6	18
168	Centimeter-Long and Large-Scale Micropatterns of Reduced Graphene Oxide Films: Fabrication and Sensing Applications. ACS Nano, 2010, 4, 3201-3208.	14.6	571
169	Surface immobilized cholera toxin B subunit (CTB) facilitates vesicle docking, trafficking and exocytosis. Integrative Biology (United Kingdom), 2010, 2, 250.	1.3	12
170	Two- and three-dimensional folding of thin film single-crystalline silicon for photovoltaic power applications. Proceedings of the National Academy of Sciences of the United States of America, 2009, 106, 20149-20154.	7.1	198
171	VISUALIZATION EX SITU OF SINGLE DNA MOLECULES INCUBATION: A FIRST STEP FOR QUANTITATIVE ANALYSIS ON MULTI-SITE DEGRADATION AND ENZYMATIC KINETICS. Surface Review and Letters, 2009, 16, 79-85.	1.1	1
172	Peptide Diffusion and Self-Assembly in Ambient Water Nanofilm on Mica Surface. Journal of Physical Chemistry B, 2009, 113, 8795-8799.	2.6	31
173	A Method for Fabrication of Graphene Oxide Nanoribbons from Graphene Oxide Wrinkles. Journal of Physical Chemistry C, 2009, 113, 19119-19122.	3.1	52
174	ORGANIC SOLVENT-ASSISTED TRANSFER PRINTING ON HYDROPHOBIC POLYMER SUBSTRATE WITH HIGH EFFICIENCY. Surface Review and Letters, 2008, 15, 763-768.	1.1	4
175	FABRICATION OF TRUE-COLOR MICROPATTERNS BY 2D STEPWISE CONTRACTION AND ADSORPTION NANOLITHOGRAPHY (SCAN). Surface Review and Letters, 2007, 14, 129-134.	1.1	1
176	INVESTIGATION ON THE MORPHOLOGY OF PRECIPITATED CHEMICALS FROM TE BUFFER ON SOLID SUBSTRATES. Surface Review and Letters, 2007, 14, 1121-1128.	1.1	6
177	Organic Solvents Mediate Self-assembly of GAV-9 Peptide on Mica Surface. Acta Biochimica Et Biophysica Sinica, 2007, 39, 285-289.	2.0	17
178	Glycerol facilitates the disaggregation of recombinant adeno-associated virus serotype 2 on mica surface. Colloids and Surfaces B: Biointerfaces, 2007, 60, 264-267.	5.0	4
179	A Simple Miniaturization Protocol to Produce Multicomponent Micro- and Nanostructures. Small, 2006, 2, 884-887.	10.0	8